Ab initio Study of HZnF†

S. Hayashi, C. Léonard,* and G. Chambaud

Université Paris-Est, Laboratoire Modélisation et Simulation Multi-Echelle MSME FRE 3160 CNRS, 5 bd Descartes, Champs-sur-Marne 77454 Marne-la-Vallée Cedex 2, France

Received: May 11, 2009; Revised Manuscript Received: October 16, 2009

On the basis of highly correlated ab initio calculations, an accurate determination of the electronic structure and of the rovibrational spectroscopy has been performed for the electronic ground state of the HZnF system. Using effective core pseudopotentials for the Zn and F atoms and associated aug-cc-pVQZ basis sets, we have calculated, at the multireference configuration interaction level including the Davidson correction, the three-dimensional potential energy surface of the $X^1\Sigma^+$ ground state. The rovibrational energy levels have been obtained variationally, and the results have been discussed and compared with existing experimental data on the ground state of the close system HZnCl, which exhibits a complicated vibration−rotation spectrum. Our analysis shows that the nature of the H-ZnF bond is quite similar to that of the H-ZnCl bond, according to their bond lengths, harmonic frequencies of the H−Zn stretching mode, and dissociation energies into H and ZnF/ZnCl. The ab initio study of the electronic ground and excited states of ZnH and ZnH^+ are also presented using similar level of calculations. Characteristic constants are given for the first bounded electronic states correlating to the first two dissociation asymptotes of the neutral and ionic diatomics.

1. Introduction

Zn is an element that is present in many chemical and biological systems, as well as in materials. It is known for its highly interesting metallic properties and also because of its innocuity contrary to the metals of the same family, Cd and Hg. For example, Zn is a common constituent in batteries, and its dissolution by acids (such as HCl) takes part in recycling processes of "mercury-free batteries".[1] Other useful application is the introduction of ZnF_2 in the composition of new glasses:[2] in that case ZnF_2 can be produced by reaction of HF with zinc and HZnF is certainly present in this process.[3] New data on this later system could be interesting for the understanding and monitoring of this reaction. Moreover, from a theoretical point of view, the existence of several abundant isotopes of Zn will give rise to specific and rather complicated rovibrational spectra for the molecules containing this element, which deserves an accurate analysis.

In the last two decades, the reactions between HCl and metal atoms have been largely investigated using matrix-isolation techniques, but to our knowledge, only a few similar analyses have been performed on the close system HF plus metal. With alkaline metals, Na and K, it is found that HCl forms the ion pair M^+HCl^-,[4,5] whereas Li leads to metal atom adducts Li:HX (X = Cl, F).[6] In contrast, by insertion of the metal in the H−Cl bound, Fe and Hg form a linear metal hydrochloride HMCl,[7−9] and Al leads to a bent compound HAlCl.[10] Recently, Macrae et al. studied the reaction of HCl with the metal atoms Zn, Cd, and Hg in solid argon matrices and identified the formation of the linear metal hydrochlorides.[11] They observed the infrared spectrum of these species and identified the three normal vibrational modes. However, the bond lengths could not be determined due to the absence of a rotational analysis. Yu et al. recorded the vibration−rotation emission spectrum of gaseous HZnCl and determined the fundamental frequency for the H−Zn stretching mode.[12] Their spectrum shows a complicated pattern that has been related to the small rotational constant and to the existence of several natural isotopologues of HZnCl. In their work, a large uncertainty remains on the H−Zn bond length. Very recently, Pulliam et al.[13] recorded the microwave spectrum of HZnCl ($X^1\Sigma^+$) and determined very accurate rotational constants and bond lengths. On the basis of RCCSD(T)/cc-pVTZ calculation, Kerkines et al. reported reliable bond lengths and harmonic frequencies for the three normal modes of the $^1\Sigma^+$ ground state[14] of HZnCl. Contrary to HZnCl, there is no existing study on HZnF.

In the present work, we report the first theoretical investigation on the ground state of HZnF, focused on its electronic structure and spectroscopic properties. Beside a comparison with HZnCl, our particular interests in such compounds containing Zn are to discuss a specific signature in their vibrational spectroscopy arising from several natural isotopes of Zn.[15] In addition, the present study is aimed at the determination of predictive data that would help HZnF to be a likely target for rovibrational experimental studies. For this reason, the rovibrational information is given for the most abundant isotopologues. Since HZnF is expected to be an ionic compound, its diatomic fragments should be carefully studied to identify the electronic states of HZnF that interact in the molecular region. The low lying states of ZnH are known,[16,17] and those of ZnF have been recently investigated.[18] We start the present study with a description of the first dissociation asymptotes of HZnF and of the correlated molecular states. The one-dimensional (1D) cuts of the potential energies for the low lying states are then reported, and the stability of the electronic states is discussed. The following section presents the three-dimensional (3D) potential energy surface (PES) of the ground state and the calculated rovibrational energy levels up to 3000 cm^{-1}. In the last section, the properties of the ground state of HZnF are compared with those of HZnCl. To help this comparison, the

† Part of the "Vincenzo Aquilanti Festschrift".

* Corresponding author. Telephone: +33.1.60.95.73.18; Fax: +33.1.60.95.73.20; E-mail: celine.leonard@univ-paris-est.fr.

10.1021/jp9043607
Published on Web 11/04/2009

potential curves and some properties of the electronic ground and first excited states of ZnH and ZnH^+ are also reported.

2. Dissociation Asymptotes and Correlated Molecular States

The interesting dissociation products of HZnF are [HZn + F] and [ZnF + H]: the Zn plus HF combination is not considered here because it involves a preliminary isomerization of the stable HZnF form. Concerning the first dissociation asymptotes of HZnF into ZnH and F and the corresponding molecular states in linear geometry, the lowest dissociation asymptote comes from a combination between the $^2\Sigma^+$ ground state of ZnH and the ^2P_u ground state of F, leading to a $^{1,3}\Sigma^+$ and a $^{1,3}\Pi$ molecular states. Then, a $^{1,3}\Sigma^+$, a $^{1,3}\Sigma^-$, a $^{1,3}\Pi$, and a $^{1,3}\Delta$ molecular states are correlated with the second asymptote involving the Zn-H($A^2\Pi$) excited state and the F(^2P_u) ground state, lying at 2.886 eV above the lowest one.[16,17] The third asymptote with the ZnH($B^2\Sigma^+$) and F(^2P_u) fragments, lying at 3.420 eV above the first one, correlates with a $^{1,3}\Sigma^+$ and a $^{1,3}\Pi$ states.[16,17] The dissociation asymptote arising from the ^4P_g first excited state of F and from the ground state of ZnH lies at 12.701 eV (averaged over the fine structure levels) above the first asymptote and is not taken into account in this study.[19] On the basis of experimental values,[16,19,20] the ionization energy from the ZnH($X^2\Sigma^+$) state to the ZnH^+($X^1\Sigma^+$) state is equal to IE(ZnH) = IE(Zn) + D_0[ZnH^+($X^1\Sigma^+$)] − D_0[ZnH($X^2\Sigma^+$)] = 9.394 + 0.85 − 2.5 ≈ 7.8 eV. Using the experimental electronic affinity of F (3.398 eV),[15] the first ionic dissociation asymptote lies at 4.4 eV above the lowest covalent one, correlating with a $^1\Sigma^+$ molecular state.

The situation of the dissociation into H and ZnF is somehow more complicated. The lowest dissociation asymptotes into H and ZnF differ only in the electronic states of ZnF,[18] because of the large excitation energy required to reach the first excited state of H (10.199 eV).[19] The resulting HZnF molecular states have the same representation in $C_{\infty v}$ symmetry group as those of the ZnF fragment with the singlet or triplet spin multiplicity due to the hydrogen electron. Thus, the lowest dissociation asymptote involving the H(^2S_g) and ZnF($X^2\Sigma^+$) fragments correlates with a $^{1,3}\Sigma^+$ state. The second to the seventh asymptotes leading to singlet states correspond to a combination of the ground state of H with two $^2\Sigma^+$, three $^2\Pi$, a $^2\Delta$, and a $^2\Sigma^-$ states of ZnF and correlate totally with two $^{1,3}\Sigma^+$, three $^{1,3}\Pi$, a $^{1,3}\Delta$, and a $^{1,3}\Sigma^-$ molecular states. Concerning the ionic dissociation asymptote ZnF^- + H^+, the electronic affinity of ZnF^- was reported to be 1.974 eV (T_0) by Moravec et al.,[21] and the ionization energy of H(^2S_g) equals 13.595 eV.[19] Thus, this ionic asymptote, correlating with a $^1\Sigma^+$ state, lies at 11.621 eV above the first covalent one.

The covalent and ionic dissociation asymptotes into HZn + F and H + ZnF, and the resulting low lying electronic states of HZnF in linear geometry are presented in Table 1 using T_e values for the bound states and vertical electronic transition energy (T_v) values for the repulsive states of ZnF.

TABLE 1: Lowest Covalent and Ionic Dissociation Asymptotes of HZnF Leading to Singlet States and the Resulting Low Lying Electronic States for Linear Geometry[a]

dissociation asymptotes	energies [eV]	molecular states
	HZn + F	
ZnH($X^2\Sigma^+$) + F(^2P_u)	0	$^{1,3}\Sigma^+$, $^{1,3}\Pi$
ZnH($A^2\Pi$) + F(^2P_u)	2.886	$^{1,3}\Sigma^+$, $^{1,3}\Pi$, $^{1,3}\Delta$, $^{1,3}\Sigma^-$
ZnH($B^2\Sigma^+$) + F(^2P_u)	3.420	$^{1,3}\Sigma^+$, $^{1,3}\Pi$
ZnH^+($X^1\Sigma^+$) + F^-(^1S_g)	4.4	$^1\Sigma^+$
	H + ZnF	
H(^2S_g) + ZnF($X^2\Sigma^+$)	0	$^{1,3}\Sigma^+$
H(^2S_g) + ZnF($B^2\Sigma^+$)	4.101	$^{1,3}\Sigma^+$
H(^2S_g) + ZnF($A^2\Pi$)	4.634 (T_v)	$^{1,3}\Pi$
H(^2S_g) + ZnF($C^2\Pi$)	4.876	$^{1,3}\Pi$
H(^2S_g) + ZnF($D^2\Sigma^+$)	6.694	$^{1,3}\Sigma^+$
H(^2S_g) + ZnF($^2\Delta/^2\Sigma^-$)	8.323 (T_v)	$^{1,3}\Delta$, $^{1,3}\Sigma^-$
H(^2S_g) + ZnF($^2\Pi$)	9.907 (T_v)	$^{1,3}\Pi$
H^+ + ZnF^-($X^1\Sigma^+$)	11.621	$^1\Sigma^+$

[a] The asymptote energies come from the most accurate experimental works at our knowledge and at the present time. In absence of experimental data, the most accurate theoretical values are taken. The equilibrium energy of the fundamental electronic states of ZnF and ZnH are taken as reference. T_e is used for the bound states of ZnF,[18] ZnF^-,[18] ZnH,[16,17] and ZnH^+,[20] and the vertical transition energy (T_v) for the repulsive states at the equilibrium geometry of the ground state of ZnF (3.337 bohr).[18] Atomic energies are averaged over the fine structure levels.[19]

3. Computational Details

3.1. Pseudo-Potentials and Basis Sets. In order to take into account relativistic effects of the Zn core electrons, the recent energy-consistent ECP10MDF effective core potential[22] represents the 10 inner electrons. The 20 outer electrons are explicitly treated via the associated aug-cc-pVQZ basis sets contracted to (14s11p11d3f2g1h)/[6s6p5d3f2g1h].[23] The energy-consistent ECP2MWB effective core potential is used for the 2 core electrons of F[24] and the 7 outer electrons are treated explicitly in the calculations, using the associated (4s5p)/[2s3p] basis sets[24] augmented with the 4d, 3f, and 2g primitives taken from the Dunning et al. correlation consistent aug-cc-pVQZ basis sets.[25,26] The hydrogen atom electron is described by the Dunning et al. correlation consistent aug-cc-pVQZ basis set.[25]

3.2. Molecular Structure Calculations. The 28 valence electrons wave functions of HZnF are optimized by state-averaged multi-configuration self-consistent-field (MCSCF) calculations[27,28] for all the singlet states of Table 1, that is, four $^1\Sigma^+$, three $^1\Pi$, a $^1\Delta$, and a $^1\Sigma^-$ states. Fourteen active molecular orbitals are constructed with the 3d, 4s, and 4p of Zn, the 2p and 3s of F, and the 1s of H. Among these 14 orbitals, 5 inner shells corresponding to the 3d of Zn are optimized but not correlated in this step. The effective active space thus consists in the (5−9)σ and (3−4)π orbitals.

Taking the MCSCF wave functions as reference, the subsequent internally contracted multi-reference-configuration-interaction (MRCI) calculations are performed only for the $X^1\Sigma^+$ electronic ground state.[29,30] The Davidson correction,[31,32] which approximates the contribution of quadruple excitation terms, has been introduced in the last step of the calculation (MRCI+Q). All electronic structure calculations are performed in C_{2v} or C_s symmetry group, using the MOLPRO program package.[33]

3.3. Spin−Orbit Coupling Terms Calculations. With the assumption that the spin−orbit couplings can be treated perturbatively to be used later in the spectroscopy calculations, the spin-orbit coupling terms can be calculated as the matrix elements of the nonrelativistic part of the Breit-Pauli operator $\hat{H}_{SO}^{BP}$ on the basis of the spin-electronic wave functions.[34] We used here the MCSCF wave functions expanded on the contracted *s*, *p*, and *d* functions of the aug-cc-pVQZ basis set for H, the contracted *s*, *p*, *d*, and *f* functions of the aug-cc-pVQZ basis set for F (without core potential for F). The 10 core electrons of Zn are represented by the ECP10MDF effective core potential and the remaining 20 electrons by the *s*, *p*, *d*, *f*, and *g* functions of the associated aug-cc-pVQZ basis sets. For all the geometries, the molecule is fixed in the *xz*-plane where the *x*-axis bisects the bond at angle θ and the *z*-axis corresponds

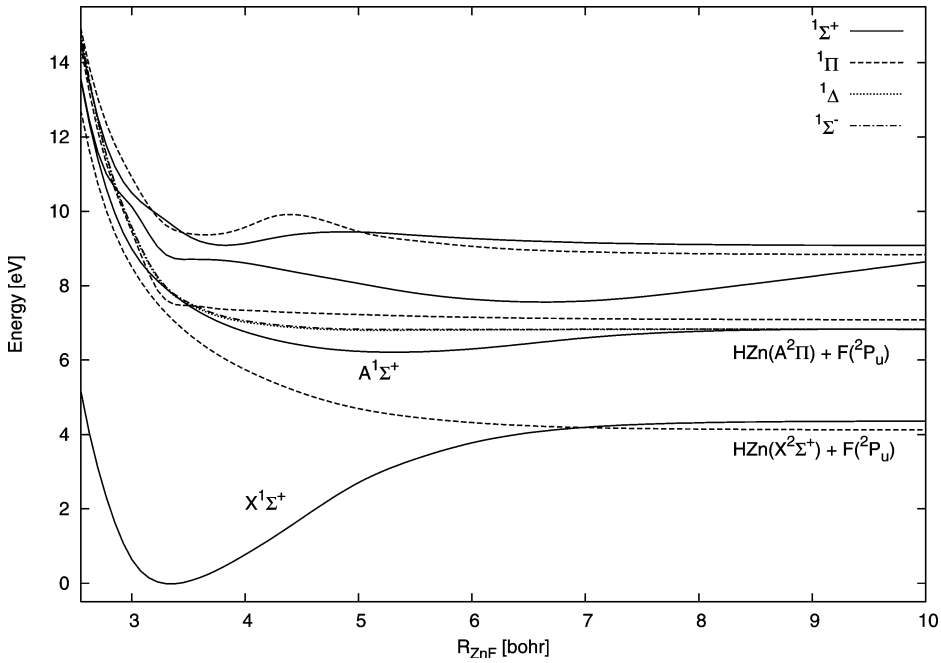

Figure 1. Potential curves of the low lying singlet states of HZnF along R_{ZnF}, in linear geometry with $R_{ZnH} = 3.014$ bohr, at the MCSCF level of theory.

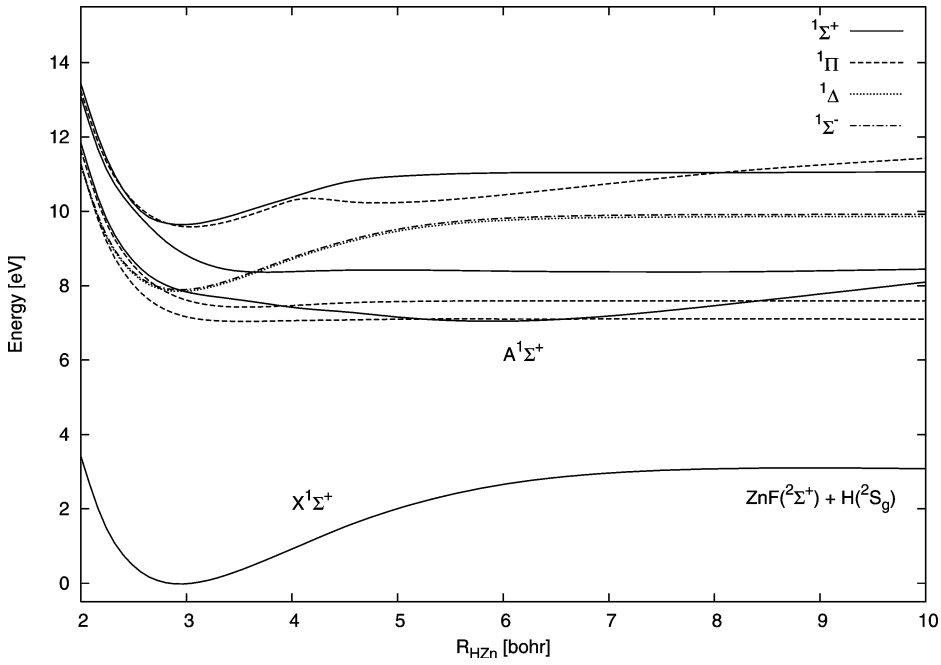

Figure 2. Potential curves of the low lying singlet states of HZnF along R_{ZnH}, in linear geometry with $R_{ZnF} = 3.337$ bohr, at the MCSCF level of theory.

to the linear molecular axis. The central atom is fixed at the reference frame origin.

4. Results

4.1. Low Lying Singlet Electronic States of HZnF. In the first step of this study, the 1D cuts of potential energy curves of the low lying singlet electronic states of HZnF are presented from the MCSCF calculations. For linear geometries, Figure 1 shows their variations with the distance R_{ZnF}. R_{HZn} is fixed at the experimental equilibrium geometry of the ZnH($X^2\Sigma^+$) state, that is, 3.014 bohr.[16] Figure 2 presents the potential curves in linear geometry along R_{HZn} with R_{ZnF} fixed at the ZnF($X^2\Sigma^+$) state calculated equilibrium geometry of 3.337 bohr.[18] In Figures 1 and 2, the electronic ground state of HZnF is clearly the lowest $^1\Sigma^+$ state, with the approximate equilibrium bond lengths of 3.35 bohr for R_{ZnF} and of 2.94 bohr for R_{HZn}.

This electronic ground state is well separated in energy from the low lying excited states. From the linear cuts shown in Figure 1, taking the minimum of the ground state as energy reference, the first $^1\Pi$ state is repulsive and lies at 7.42 eV, and the minimum of the $A^1\Sigma^+$ state is found at 6.20 eV, respectively. In these linear cuts, the first two $^1\Sigma^+$ excited states have a flat minimum at long distances coming from interactions between them. In contrast, almost all the other excited states are repulsive.

In Figure 2, the asymptote order is coherent with the excited electronic states energy order of ZnF for $R_{ZnF} = 3.337$ bohr.[18]

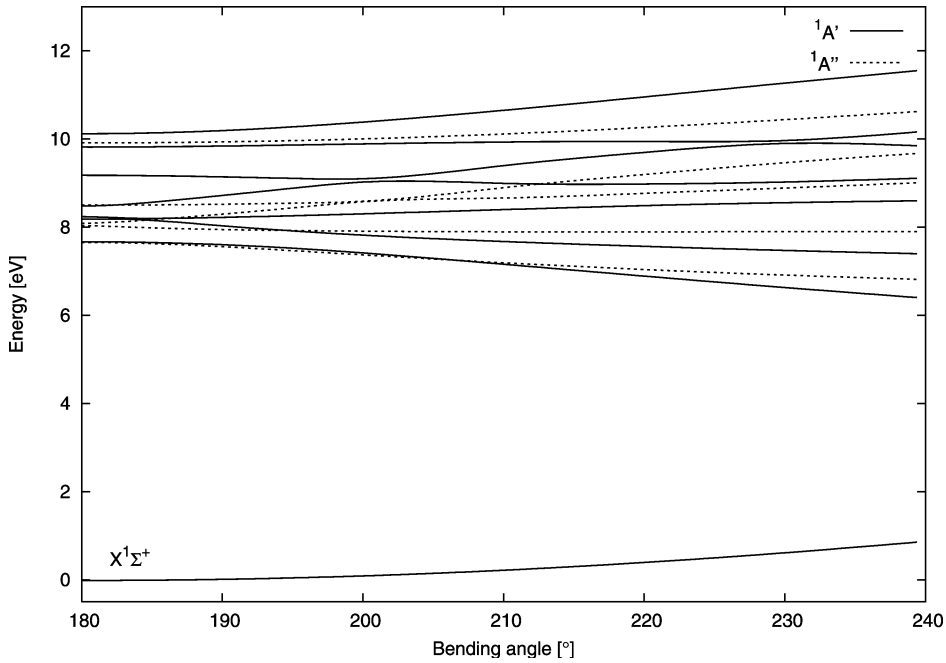

Figure 3. Potential curves of the low lying singlet states of HZnF, along the bending angle θ, at the MCSCF level of theory.

The HZnF A$^1\Sigma^+$ state is separated at least by 7.05 eV from the minimum of the ground state with an equilibrium HZn bond length around 6 bohr. The first two excited $^1\Pi$ states are repulsive, and the first $^1\Delta$ and $^1\Sigma^+$ have a minimum for $R_{HZn} \approx$ 3 bohr similarly to the ground state. In Figures 1 and 2, the long-range minima of the $^1\Sigma^+$ excited states are the sign of a strong ionic contribution in their corresponding wave functions (as an example, see the discussion in section II of ref 18).

The variations of the potential curves along the bending angle θ from 180 to 240° are presented in Figure 3 for the low lying singlet states of HZnF. R_{ZnH} is fixed at 2.942 bohr and R_{ZnF} at 3.344 bohr. The doubly degenerate $^1\Pi$ and $^1\Delta$ states split into $^1A'$ and $^1A''$ components. The ground state $^1\Sigma^+$ has its minimum in linear geometry and is again found to be isolated in energy for this bending angle range (the first excited states, $^1A'$ and $^1A''$ from the first $^1\Pi$ state, lying at 7.67 eV above the ground state for $\theta = 180°$). The higher excited state potentials have their minimum for linear geometries, whereas the potential energies of the lower excited states decrease when θ varies from 180 to 240°. These behaviors are likely to arise from the avoided crossings between two $^1A'$ states at $\theta \approx 200$ and $\approx 230°$, and between two $^1A''$ states at $\theta \approx 200°$.

4.2. Potential Energy Surface of the $X^1\Sigma^+$ Ground State. According to the complicated interactions between the low lying states of ZnF,[18] we had to include many low lying states of HZnF at the MCSCF level to obtain an accurate description of the ground state of HZnF in the MRCI+Q calculations. This is the sign that the X$^1\Sigma^+$ electronic ground state is not monoconfigurational, despite its energetic isolation. We found that the major configuration $5\sigma^2\ 6\sigma^2\ 3\pi^4$ has a squared root weight in the MCSCF wave function between 0.953 and 0.937 for $R_{HZn} \in$ [2.4;3.6] bohr and between 0.969 and 0.922 for $R_{ZnF} \in$ [2.75;4.0] bohr. This last value indicates that the use of monoconfigurational coupled-cluster theory as in the work of Kerkines et al.[14] for HZnCl is questionable.

The MRCI+Q calculations have been carried out in C_s symmetry group for 31 geometries (19 linear and 12 non linear), within variations of R_{ZnH}, R_{ZnF}, and of the bending angle θ, corresponding to an energy variation of approximately 10,000 cm^{-1} from the equilibrium energy, which corresponds to $2.31 \le R_{ZnH} \le 3.56$ bohr, $2.89 \le R_{ZnF} \le 3.89$ bohr, and $180 \le \theta \le 220°$.

In order to give an analytical representation of the potential energy surface valid within the above geometry range, the resulting energy values have been fitted by the following polynomial expansion up to the fourth order of displacements of three internal coordinates, R_{ZnH}, R_{ZnF}, and θ.

$$V(\Delta R_{ZnH}, \Delta R_{ZnF}, \Delta\theta) = \sum_{i,j,k} C_{ijk} (\Delta R_{ZnH})^i (\Delta R_{ZnF})^j (\Delta\theta)^k$$

$$\Delta R_{ZnH} = R_{ZnH} - R_{ZnH}^{eq}$$

$$\Delta R_{ZnF} = R_{ZnF} - R_{ZnF}^{eq}$$

$$\Delta\theta = \theta - \pi$$

where $0 \le i,j,k \le 4$ and $0 \le i + j + k \le 4$. k is restricted to even values in order to conserve the symmetry of the bending coordinate. The equilibrium geometry, for which the first derivatives of the PES are equal to zero, is taken as reference. Twenty-two expansion coefficients, C_{ijk}, optimized by a least-squares-fitting, with a root-mean-square of 1.37 cm^{-1}, are listed in Table 2 with the R_{ZnH}^{eq} and R_{ZnF}^{eq} values. At this equilibrium geometry, the dipole moment has been calculated at the MRCI level, using the center of mass of the molecule as the coordinate origin, and equals 0.775 au corresponding to the $H^{\delta+}ZnF^{\delta-}$ polarity, whereas this X$^1\Sigma^+$ state is connected to a covalent asymptote.

In order to complete the study, we have determined the PES from the same geometries but the energies have been computed with the CCSD(T) method.[35,36] We noticed that the T_1 diagnostic has values close to the CCSD(T) validity limit of 0.02[37] (even larger for $R_{ZnH} > 3.20$ bohr or $R_{ZnF} > 3.60$ bohr or $\theta > 220°$). A similar analytical function of the PES has been obtained by the

TABLE 2: Polynomial Expansion Coefficients C_{ijk} (au) of the Ground $^1\Sigma^+$ PES of HZnF from the Fit of MRCI+Q Energy Points, with Its Equilibrium Geometry[a]

	coefficients		coefficients
C_{000}	−251.269 474 15	C_{012}	−0.017 647 48
C_{200}	0.081 872 98	C_{400}	0.032 206 86
C_{110}	−0.004 037 14	C_{310}	0.000 749 14
C_{020}	0.135 052 05	C_{220}	0.002 041 96
C_{002}	0.032 092 12	C_{130}	0.000 653 78
C_{300}	−0.069 476 24	C_{040}	0.080 450 24
C_{210}	−0.000 326 69	C_{202}	0.006 202 43
C_{120}	0.000 507 88	C_{112}	0.010 176 17
C_{030}	−0.142 813 62	C_{022}	0.012 807 44
C_{102}	−0.012 854 83	C_{004}	−0.002 400 91
R_{ZnH}^{eq}	2.802 (bohr)	R_{ZnF}^{eq}	3.269 (bohr)
μ_e	0.775 (au)		

[a] C_{000} is the MRCI+Q energy at equilibrium. The equilibrium dipole moment was calculated at the MRCI level.

TABLE 3: Polynomial Expansion Coefficients C_{ijk} (au) of the Ground $^1\Sigma^+$ PES of HZnF from the Fit of CCSD(T) Energy Points, with Its Equilibrium Geometry[a]

	coefficients		coefficients
C_{000}	−251.373 290 30	C_{012}	−0.018 376 01
C_{200}	0.082 346 28	C_{400}	0.032 078 16
C_{110}	−0.003 801 64	C_{310}	0.000 400 26
C_{020}	0.135 715 71	C_{220}	0.001 828 04
C_{002}	0.033 367 95	C_{130}	−0.000 014 29
C_{300}	−0.070 192 07	C_{040}	0.078 915 31
C_{210}	−0.000 589 55	C_{202}	0.005 471 10
C_{120}	0.000 663 02	C_{112}	0.008 784 58
C_{030}	−0.143 428 55	C_{022}	0.011 884 96
C_{102}	−0.013 257 08	C_{004}	−0.002 981 46
C_{006}	0.000 05		
R_{ZnH}^{eq}	2.800 (bohr)	R_{ZnF}^{eq}	3.254 (bohr)

[a] C_{000} is the CCSD(T) energy at equilibrium.

same fitting procedure as above. The resulting coefficients are given in Table 3.

Using the SURFIT program,[38] we have deduced, from the MRCI+Q and CCSD(T) PES derivatives at the minimum, the harmonic frequencies of the three normal modes ω_1, ω_2, and ω_3 for all natural isotopologues of $HZn^{19}F$ (Table 4). Decompositions of the stretching Q_1 and Q_3 normal modes into displacements of the internal coordinates ΔR_{ZnH} and ΔR_{ZnF} are shown in Table 5. It appears that the Q_1 and Q_3 normal modes are almost localized on the stretching of the ZnH and ZnF bonds respectively. The ω values differ within 10 cm^{-1} between the CCSD(T) and MRCI+Q results.

TABLE 5: Decompositions of the Stretching Normal Modes Q_1 and Q_3 into the Displacements of Internal Coordinates ΔR_{ZnH} and ΔR_{ZnF} for the Most Abundant Isotopologue $H^{64}ZnF$ from MRCI+Q PES

normal modes	ΔR_{ZnH}	ΔR_{ZnF}
Q_1	0.9984	−0.0564
Q_3	0.0193	0.9998

4.3. Rovibrational Levels of the $X^1\Sigma^+$ Ground State. For a linear triatomic molecule, there is no rotation around the molecular axis (fixed to the z-axis). Thus, the projection of the total angular moment on the z-axis, $\hat{J}_z$, has a contribution only from the z component of the vibrational angular moment, $\hat{l}_z$, if there is no angular nor electron spin contribution as for a $^1\Sigma^+$ electronic state. The quantum number l, associated with $\hat{l}_z$, can be related to the quantum number of the bending vibrational mode υ_2 as follows: $l = \pm\upsilon_2, \pm(\upsilon_2-2), ..., \pm2, 0$ (for even υ_2) or $\pm\upsilon_2, \pm(\upsilon_2-2), ..., \pm1$ (for odd υ_2). In the case of the $^1\Sigma^+$ ground state of HZnF, the rovibrational levels are characterized by the $\hat{J}_z$ quantum number K with $|K| = |l| = 0, 1, 2$. Using the RVIB3 program[39] with the previously fitted MRCI+Q and CCSD(T) PESs, the rovibrational energy levels of the HZnF $X^1\Sigma^+$ state have been computed variationally up to 3000 cm^{-1} from the zero point energy (ZPE) for the main isotopologue $H^{64}ZnF$. Thirteen harmonic oscillator eigenfunctions for each stretching mode and 70 associated Legendre polynomials for the bending mode were involved in the basis set. The primitive set of integration points contains 14 points for each stretching modes and 94 for the bending one. The optimized rovibrational levels are given in Tables 6 and 7 for $J = 0$, 1, and 2. The only resonances are found between the (1,0,1) and (0,0,4) levels around 2690 cm^{-1} from the ZPE. From the harmonic frequencies given in Table 4, no additional resonance is expected for other isotopologues. The CCSD(T) and MRCI+Q methods lead to comparable rovibrational energy levels. The larger differences concern the levels involving excitation of the bending mode.

In order to help any experimental rovibrational spectroscopic analysis of the electronic ground state of HZnF, the variational rotational constants and some vibrational energies are given in Table 8 for the most abundant isotopologues of the triatomic molecule.

4.4. Electronic Transitions and Spin−Orbit Coupling. In order to complete the study of the electronic ground state of HZnF, we investigated the electronic transitions that can occur between the $X^1\Sigma^+$ ground state and excited $^1\Sigma^+$ and $^1\Pi$ states. Table 9 gives the transition energies and dipole moments of the first allowed transitions from MRCI+Q and MRCI calcula-

TABLE 4: Harmonic Frequencies ω_1, ω_2, and ω_3 for All the Natural Isotopologues of $HZn^{19}F$ and the Main Isotopologues of $HZn^{35}Cl$

	method	isotopologues	ω_1 [cm^{-1}]	ω_2 [cm^{-1}]	ω_3 [cm^{-1}]
HZnF($^1\Sigma^+$), This work	MRCI+Q	$H^{64}ZnF$	2089.80	484.14	696.28
		$H^{66}ZnF$	2089.25	483.77	693.94
		$H^{67}ZnF$	2088.99	483.60	692.82
		$H^{68}ZnF$	2088.74	483.43	691.73
		$H^{70}ZnF$	2088.26	483.10	689.63
This work	CCSD(T)	$H^{64}ZnF$	2095.77	494.20	698.02
		$H^{66}ZnF$	2095.22	493.82	695.68
		$H^{67}ZnF$	2094.96	493.64	694.55
		$H^{68}ZnF$	2094.71	493.47	693.46
		$H^{70}ZnF$	2094.22	493.14	691.36
HZnCl($^1\Sigma^+$), Kerkines[a]	RCCSD(T)	$H^{64}Zn^{35}Cl$	2008.2	421.2	431.7
		$H^{66}Zn^{35}Cl$	2007.7	420.9	429.4
		$H^{68}Zn^{35}Cl$	2007.2	420.6	427.3

[a] Taken from ref 14, calculated at the RCCSD(T)/cc-pVTZ level.

TABLE 6: Rovibrational Levels (cm^{-1}) of the Ground $^1\Sigma^+$ State for the Main Isotopologue $H^{64}ZnF$ Using the MRCI+Q PES

(v_1, v_2, v_3)	$J=0$ $\|K\|=0$	$J=1$ $\|K\|=0$	$J=1$ $\|K\|=1$	$J=2$ $\|K\|=0$	$J=2$ $\|K\|=1$	$J=2$ $\|K\|=2$
(0,0,0)	0[a]	0.7079		2.1240		
(0,1,0)			474.5		475.9	
(0,0,1)	684.8	685.5		686.9		
(0,2,0)	938.6	939.3		940.7		950.2
(0,1,1)			1157.9		1159.3	
(0,0,2)	1360.8	1361.5		1362.9		
(0,3,0)			1404.6		1406.0	
(0,2,1)	1620.5	1621.2		1622.6		1632.1
(0,1,2)			1832.5		1833.9	
(0,4,0)	1860.2	1860.9		1862.4		1871.8
(1,0,0)	2000.8	2001.5		2002.9		
(0,0,3)	2029.5	2030.2		2031.6		
(0,3,1)			2085.0		2086.4	
(0,2,2)	2293.7	2294.4		2295.8		2305.4
(0,5,0)			2317.8		2319.2	
(1,1,0)			2465.5		2467.0	
(0,1,3)			2502.4		2503.8	
(0,4,1)	2539.2	2539.9		2541.3		2550.8
(1,0,1)	2686.4	2687.1		2688.5		
(0,0,4)	2690.4	2691.1		2692.4		
(0,3,2)			2757.0		2758.4	
(0,6,0)	2765.0	2765.7		2767.2		2776.7
(1,2,0)	2920.1	2920.8		2922.2		2931.4
(0,2,3)	2966.6	2967.3		2968.7		2978.2
(0,5,1)			2995.2		2996.6	
...						
(2,0,0)	3950.8	3951.6		3953.0		

[a] Zero rovibrational level at 1853.397 cm^{-1} above the equilibrium energy.

TABLE 7: Rovibrational Levels (cm^{-1}) of the Ground $^1\Sigma^+$ State for the Main Isotopologue $H^{64}ZnF$ Using the CCSD(T) PES

(v_1, v_2, v_3)	$J=0$ $\|K\|=0$	$J=1$ $\|K\|=0$	$J=1$ $\|K\|=1$	$J=2$ $\|K\|=0$	$J=2$ $\|K\|=1$	$J=2$ $\|K\|=2$
(0,0,0)	0[a]	0.7143		2.1428		
(0,1,0)			483.5		484.9	
(0,0,1)	686.2	686.9		688.3		
(0,2,0)	956.0	956.7		958.1		967.8
(0,1,1)			1168.0		1169.4	
(0,0,2)	1363.2	1363.9		1365.3		
(0,3,0)			1430.1		1431.5	
(0,2,1)	1638.8	1639.5		1640.9		1650.7
(0,1,2)			1843.4		1844.8	
(0,4,0)	1893.1	1893.9		1895.3		1905.0
(1,0,0)	2003.2	2004.0		2005.4		
(0,0,3)	2032.7	2033.4		2034.8		
(0,3,1)			2111.2		2112.6	
(0,2,2)	2312.7	2313.4		2314.8		2324.5
(0,5,0)			2357.8		2359.3	
(1,1,0)			2476.1		2477.5	
(0,1,3)			2514.0		2515.4	
(0,4,1)	2572.5	2573.2		2574.6		2584.4
(1,0,1)	2690.1	2690.8		2692.2		
(0,0,4)	2694.0	2694.7		2696.0		
(0,3,2)			2783.5		2784.9	
(0,6,0)	2811.6	2812.3		2813.7		2823.5
(1,2,0)	2938.2	2938.9		2940.3		2949.7
(0,2,3)	2986.1	2986.8		2988.2		2998.0
(0,5,1)			3035.4		3036.9	
...						
(2,0,0)	3952.4	3953.1		3954.5		

[a] Zero rovibrational level at 1866.043 cm^{-1} above the equilibrium energy.

tions, respectively. These transitions are rather intense and can be observed in the VUV domain (from 8.4 eV). From Figures 1 and 2, we can expect that they all lead to the dissociation of HZnF into HZn + F(^2P_u) fragments. The vertical energy positions of the first $^3\Sigma^+$ and $^3\Pi$ states are also given in Table 9.

Zn is a heavy atom with experimental spin−orbit splittings equal to 190 and 389 cm^{-1} in the first ^3P_u state[19] and we can expect large effect of the spin−orbit coupling in the rovibronic levels of Zn compounds. However, the first triplet state of HZnF, that is, a $^3\Sigma^+$ state, lies at 7.386 eV from the equilibrium position of the electronic ground state. In this situation, the effect of the spin−orbit interaction between the electronic ground state and excited states, which is at most equal to 130 cm^{-1}, gives negligible perturbations of the $X^1\Sigma^+$ potential surface (less than 1 cm^{-1}). Using the same kind of calculations for Zn, the spin−orbit splittings equal to 189 and 378 cm^{-1} in the first ^3P_u state compare very well with the experimental data.[19]

For information, the values of the spin−orbit coupling terms between the first electronic states of HZnF, calculated for the equilibrium geometry of the electronic ground state, are given in Table 10.

TABLE 8: MRCI+Q Variational Rotational Constant and Some Vibrational Energy Levels for the Natural Isotopologues of HZnF (in cm^{-1})

isotopologues	B_0	$1\nu_1$	$1\nu_3$	$1\nu_2^1$	$2\nu_2^0$
$H^{64}ZnF$	0.3540	2000.8	684.8	474.5	938.6
$H^{66}ZnF$	0.3520	2000.3	682.6	474.1	937.9
$H^{67}ZnF$	0.3510	2000.1	681.5	474.0	937.6
$H^{68}ZnF$	0.3501	1999.9	680.4	473.8	937.3
$H^{70}ZnF$	0.3482	1999.4	678.4	473.5	936.7

TABLE 9: First Vertical Electronic Transitions from the Minimum of the $X^1\Sigma^+$ Electronic Ground State[a]

electronic states	transition energy [eV]	transition dipole moment [au]
$C^1\Sigma^+$	9.065	0.8102
$B^1\Sigma^+$	9.631	0.6560
$A^1\Pi$	8.404	0.7309
$b^3\Pi$	8.400	
$a^3\Sigma^+$	7.386	

[a] The energies have been determined from MRCI+Q calculations. The transition dipole moments with the X state are expectation values using MRCI wavefunctions.

5. Discussion

5.1. ZnH and ZnH^+. The analysis of the ground state of HZnF requires also information about the electronic ground states of ZnH and ZnH^+. Indeed, these diatomic molecules have been already investigated both in theoretical and experimental works,[16,17,20,40−47] however we decided to complete the studies of both systems by exploring the excited electronic states. The electronic calculations were performed using the same basis set as for HZnF, that is, 21 and 20 valence electrons for ZnH and ZnH^+, respectively, with 11 active molecular orbitals constructed on the 3d, 4s, 4p, and 5s of Zn and 1s of H. Thus, the effective active space is formed by the $(3-7)\sigma$, $(2-3)\pi$, and 1δ molecular orbitals. As for HZnF, the MCSCF wave functions are taken as reference for the subsequent MRCI+Q calculations. All electronic structure calculations for the diatomics are performed in the C_{2v} symmetry group, using the MOLPRO program package.[33]

TABLE 10: Spin−Orbit Couplings Terms (cm^{-1}), i.e., Expectation Values of the Breit-Pauli Operator,[34] Larger than 5 cm^{-1} between the First Electronic States of HZnF, Calculated at the Equilibrium Geometry of $X^1\Sigma^+$

spin-electronic states	$b^3\Pi_x(S_z = 1)$	$b^3\Pi_x(S_z = 0)$
$X^1\Sigma^+(S_z = 0)$	−129.29	
$B^1\Sigma^+(S_z = 0)$	−40.32	
$A^1\Pi_y(S_z = 0)$		$-i$155.26
$b^3\Pi_y(S_z = 1)$	i159.01	

With the help of NUMEROV algorithm,[48] the spectroscopic constants are deduced from the MRCI+Q potentials and are listed in Table 11.

Our calculated values show reasonable agreements with the previous ones and the ionization energy from $ZnH(X^2\Sigma^+)$ to $ZnH^+(X^1\Sigma^+)$ is calculated to be 7.684 eV (T_0), comparing well with the experimental value of 7.8 eV.[16,19,20] Thus, we can confirm the energy position of the ionic dissociation asymptote of $HZn^+ + F^-$.

In Figures 4 and 5, the lower electronic states of ZnH and ZnH^+ correlating to the first two dissociation asymptotes are displayed. The lowest dissociation asymptote of ZnH comes from a combination of the $Zn(^1S_g)$ and $H(^2S_g)$ ground states, correlating with a $^2\Sigma^+$ molecular state. Then, the second asymptote lies at 4.038 eV above the first one and corresponds to the excitation of Zn into the ^3P_u state (the value is averaged over the fine structure levels for the ^3P_u state).[19] Figure 4 and Table 11 show that the $X^2\Sigma^+$ state is well isolated with a small dissociation energy of less than 1 eV. The first excited state of ZnH is the $A^2\Pi$ state associated with an equilibrium geometry close to that of the ground state at ≈3 bohr. The $B^2\Sigma^+$ state has a flatter minimum at ≈4.3 bohr and crosses the A state around 3.75 bohr. The quartet states are repulsive. Inspection of the dipole moments of these three electronic states at their equilibrium geometries indicates that the $X^2\Sigma^+$ state is almost covalent.

Concerning ZnH^+, the lowest dissociation asymptote corresponds to the combination of $Zn^+(3d^{10}4s: {}^2S_g)$ and $H(^2S_g)$

TABLE 11: Characteristic Constants of the Low Lying Bounded States of ZnH and ZnH^+ Cation

states	method	R_e [bohr]	$\omega_e/\omega_e x_e$ [cm^{-1}]	D_e [eV]	T_e [eV]	μ_e [au]
			ZnH			
$X^2\Sigma^+$						
This work[a]	MRCI+Q	2.997	1621.6/53.9 (^{64}ZnH) 1621.2/53.8 (^{66}ZnH) 1621.0/53.8 (^{67}ZnH) 1620.9/53.8 (^{68}ZnH)	0.940	0	0.016
Kerkines[14]	RCCSD(T)	3.001		0.919		0.232
Jamorski[40]	CI	3.037	1647	0.82	0	
Chong[b]	SDCI	2.958	1775	1.00	0	0.297
	CPF	3.005	1622	1.01	0	0.249
Shayesteh[43]	exp	3.011	1603.2/50.5			
Urban[44]	exp		1615.7/59.61 (^{64}ZnH) 1615.3/59.58 (^{66}ZnH) 1615.1/59.57 (^{67}ZnH) 1615.0/59.56 (^{68}ZnH)			
Stenvinkel[17]	exp	3.014	1607.6/55.14		0	
Huber[16]	exp			0.85[c]		
$A^2\Pi$						
This work	MRCI+Q	2.851	1906.5/40.0	2.039	2.888	0.718
Jamorski	CI	2.874	1875	1.98	2.88	
Stenvinkel	exp	2.857	1910.2/40.8		2.886	
$B^2\Sigma^+$						
This work	MRCI+Q	4.295	1029.2/16.5	1.440	3.470	−0.025
Jamorski	CI	4.297	1046	1.48	3.35	
Stenvinkel	exp	4.295	1020.7/16.5		3.420	
$C^2\Sigma^+$						
Jamorski	CI	2.882	1825	1.56	5.01	
Khan[45]	exp	2.891	1824/48		5.094	
			ZnH^+			
$X^1\Sigma^+$						
This work	MRCI+Q	2.861	1950.6/65.7	2.488	0	
Greene[47]	CCSD(T)	2.872	1878			
Schilling[46]	GVB-DCCI	2.919	1868	2.271		
Bengtsson[20]	exp	2.863	1916/39	2.5[c]	0	
$A^1\Sigma^+$						
This work	MRCI+Q	3.297	1245.8/35.4	2.583	5.896	
Bengtsson	exp	3.243	1365/15		5.790	
$b^3\Pi$						
This work	MRCI+Q	3.306	1205.5/26.0	1.107	7.363	
$B^1\Pi$						
This work	MRCI+Q	3.705	997.2/88.6	0.430	8.107	

[a] Absolute energy values calculated at the minimum of the ground state; −227.01988183 au for ZnH and −226.74448416 au for ZnH^+. The dipole moment of ZnH is calculated at the MRCI level. [b] Taken from refs 41 and 42 using the [9s7p4d3f1g] and [4s3p2d] contracted Gaussian basis sets for Zn and H respectively, with included relativistic effects. Only the dipole moments were calculated with the [9s7p4d] and [4s3p] contracted Gaussian basis sets. [c] Extrapolated D_0 value.

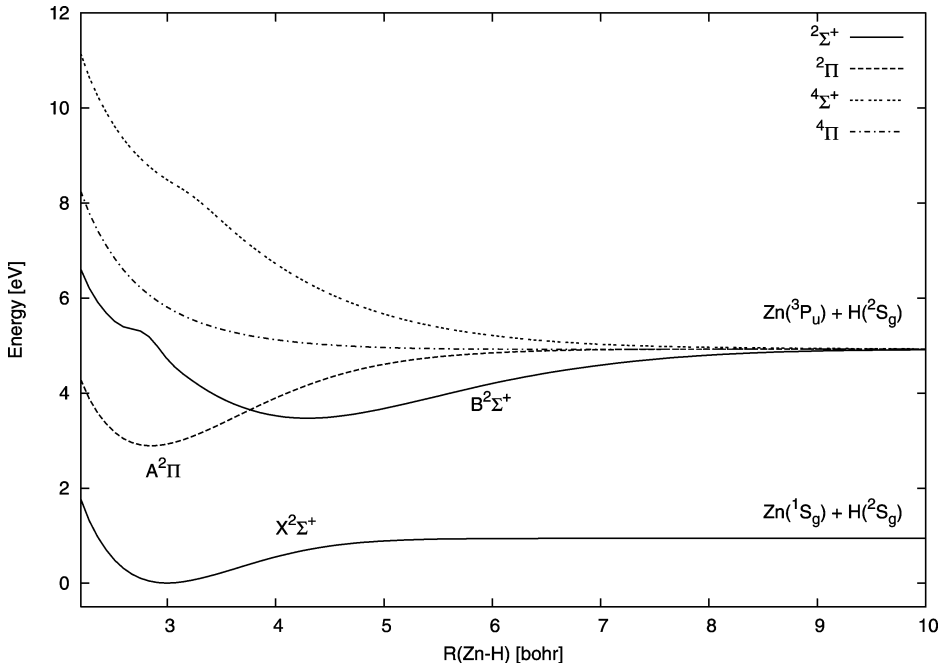

Figure 4. Potential energy curves of the low lying states of ZnH, correlated with the two lowest asymptotes, at the MRCI+Q level of theory, along R_{ZnH}.

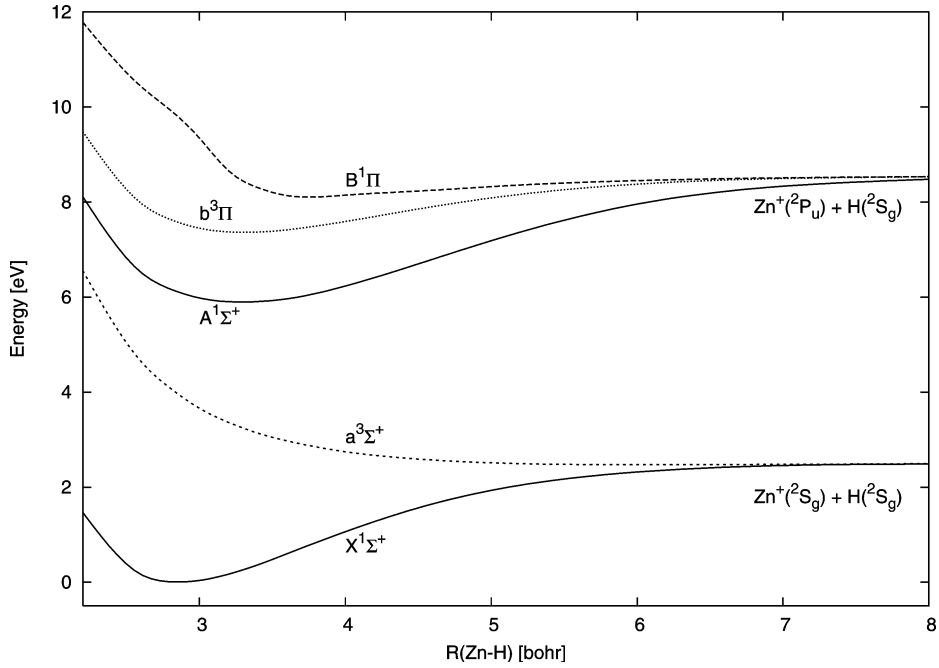

Figure 5. Potential energy curves of the low lying states of ZnH^+ at the MRCI+Q level of theory along R_{ZnH}.

fragments, lying at 9.394 eV above the lowest one of the neutral ZnH, according to the ionization energy of Zn,[19] and correlates with a $^1\Sigma^+$ and a $^3\Sigma^+$ molecular states. The second asymptote resulting from the $Zn^+(3d^{10}4p^1: {}^2P_u)$ and $H(^2S_g)$ states lies at 6.065 eV (averaged over the fine structure levels) above the first one, corresponding to the excitation energy of the $Zn^+(^2P_u)$ state.[19] This second asymptote correlates with a $^{1,3}\Sigma^+$ and a $^{1,3}\Pi$ molecular states. From Figure 5 and Table 11, we can see that all the bounded states, that is, the $X^1\Sigma^+$, $A^1\Sigma^+$, and $b^3\Pi$ states, have an equilibrium geometry around 3 bohr. The first $a^3\Sigma^+$ excited state is repulsive, but does not cross any excited state due to the large energy difference between the first two dissociation asymptotes. No predissociation phenomenon involving this state is expected.

For both diatomics, the spin−orbit coupling terms are given in Tables 12 and 13 to complete the information for these systems. The ground potential curves are almost unperturbed by the spin−orbit interactions with higher states for ZnH and ZnH^+. The strong change, with R_{ZnH}, of the spin−orbit coupling terms involving the $X^2\Sigma^+$ and $B^2\Sigma^+$ states, as shown in Table 12, is the sign of a large electronic interaction between them.

5.2. Comparison Between HZnF and HZnCl. We summarize the spectroscopic constants of the ground states of HZnF, HZnCl, and of their diatomic fragments in Table 14. According to the bond length between H and Zn, the harmonic frequency of the H−Zn stretching mode, and the dissociation energy into H and ZnX (X = F, Cl), the H-ZnX bonds are found to be similar in HZnCl and HZnF. The corresponding constants listed

TABLE 12: Spin−Orbit Couplings Terms, i.e., Expectation Values of the Breit-Pauli Operator,[34] Larger than 3 cm^{-1} between the First Electronic Doublet States of ZnH at Pertinent Geometries

R_{ZnH} [bohr]	2.851	2.997	3.75[a]	4.295
$\langle X^2\Sigma^+(S_z = 1/2)\|\hat{H}_{SO}^{BP}\|A^2\Pi_x(S_z = -1/2)\rangle$ [cm^{-1}]	149.98	140.95	90.93	60.40
$\langle A^2\Pi_y(S_z = -1/2)\|\hat{H}_{SO}^{BP}\|A^2\Pi_x(S_z = -1/2)\rangle$ [cm^{-1}]	$-i$175.20	$-i$174.67	$-i$165.80	$-i$155.79
$\langle B^2\Sigma^+(S_z = 1/2)\|\hat{H}_{SO}^{BP}\|A^2\Pi_x(S_z = -1/2)\rangle$ [cm^{-1}]	4.72	15.61	77.09	91.24

[a] The intersection of the $A^2\Pi$ and $B^2\Sigma^+$ states of ZnH is at approximately 3.75 bohr.

TABLE 13: Spin−Orbit Couplings Terms (cm^{-1}), i.e., Expectation Values of the Breit-Pauli Operator,[34] Larger than 3 cm^{-1} between the First Electronic States of ZnH$^+$, Calculated at the Equilibrium Geometry of $X^1\Sigma^+$

spin-electronic states	$b^3\Pi_x(S_z = 1)$	$b^3\Pi_x(S_z = 0)$	$A^1\Pi_x(S_z = 0)$
$X^1\Sigma^+(S_z = 0)$	−89.98		
$B^1\Sigma^+(S_z = 0)$	−174.02		
$A^1\Pi_y(S_z = 0)$		$-i$250.18	
$b^3\Pi_y(S_z = 1)$	i254.65		
$a^3\Sigma^+(S_z = 0)$	−105.17		
$a^3\Sigma^+(S_z = 1)$			104.66

TABLE 14: Spectroscopic Constants of the Ground States of $H^{64}Zn^{19}F$, $H^{64}Zn^{35}Cl$, and Their Diatomic Fragments from the Most Accurate Experimental and Theoretical Data

molecule	methods	R_e [bohr]	ω [cm^{-1}]	D_e [eV]
	H···ZnF/ZnCl			
HZnF($X^1\Sigma^+$)				
This work	MRCI+Q	2.802	2089.8	3.68
HZnCl($X^1\Sigma^+$)				
Kerkines[a]	RCCSD(T)	2.833	2008.2	3.56
Pulliam[b]	exp	2.844		
ZnH($X^2\Sigma^+$)				
This work	MRCI+Q	2.997	1621.6	0.94
Shayesteh[c]	exp	3.011	1603.2	
Huber[d]	exp			0.85 (D_0)
ZnH^+($X^1\Sigma^+$)				
This work	MRCI+Q	2.861	1950.6	2.49
Bengtsson[e]	exp	2.863	1916	2.5 (D_0)
	HZn···F/Cl			
HZnF($X^1\Sigma^+$)				
This work	MRCI+Q	3.269	696.3	5.77
HZnCl($X^1\Sigma^+$)				
Kerkines[a]	RCCSD(T)	3.929	431.7	4.79
Pulliam[b]	exp	3.936		
Yu[f]	exp	3.938		
ZnF($X^2\Sigma^+$)				
Hayashi[g]	MRCI+Q	3.337	638.6	3.03
Flory[h]	exp	3.341	631	3.12
ZnCl($X^2\Sigma^+$)				
Kerkines[a]	RCCSD(T)	4.010		2.15
Tenenbaum[i]	exp	4.025	392.1	2.73 (D_0)

[a] Taken from ref 14, calculated at the RCCSD(T)/cc-pVTZ level. [b] Taken from ref 13, from the rotational spectrum. [c] Taken from ref 43, from high resolution infrared emission spectrum. [d] Taken from ref 16, extrapolated D_0 value. [e] Taken from ref 20, extrapolated D_0 value. [f] Taken from ref 12. [g] Taken from ref 18, calculated at the MRCI+Q level, using the atomic pseudopotentials for Zn and F with the associated aug-cc-pVQZ basis sets. [h] Taken from ref 49, from the rotational spectrum. [i] Taken from ref 50, from the rotational spectrum.

in Table 14 for the ground states of ZnH and ZnH^+ indicate that the structures of the H-ZnX and $[Zn-H]^+$ bonds are almost identical. Concerning the HZn-X bonds, the lengths are commonly shorter by 2% in triatomic molecules compared with the diatomic fragments.

The equilibrium dipole moment of the HZnF ground state, obtained to be 0.775 au at the MRCI level, is quite similar to the value for HZnCl (0.700 au).[14] From the Mulliken population analysis using the cc-pVTZ basis set, the charges on the H, Zn, and F atoms are estimated, respectively, to be $-0.23e$, $+0.85e$, and $-0.62e$, confirming the ionic nature, $[HZn]^{\delta+}$ $F^{\delta-}$, of the electronic ground state.

Table 4 shows also the harmonic frequencies of the three normal modes for various isotopologues of HZnF and $HZn^{35}Cl$. The harmonic frequency ω_1 of the H−Zn stretching mode is quite similar between HZnF and HZnCl. In contrast to the close values of ω_2 and ω_3 in HZnCl, the bending and the Zn−F stretching modes of HZnF differ by more than 200 cm^{-1}. Thus, the rovibrational spectrum of HZnF may be less complicated than the one of HZnCl. For both molecules, we find that the values of ω_3 associated with the Zn-X stretching mode have a larger dependence on the Zn isotopes than those of ω_1 and ω_2, for which normal coordinates are dominated by the light H atom.

For $H^{64}Zn^{35}Cl$, the experimental energies for the vibrational levels only concern $\nu_1 = 1966.87$ cm^{-1} and $2\nu_1 = 3923.72$ cm^{-1}.[12] The anharmonicity of the ZnH stretching mode is then very small. For $H^{64}ZnF$, the variational values from Table 6 are 2000.8 cm^{-1} and 3950.8 cm^{-1} for ν_1 and $2\nu_1$, respectively, showing also a small anharmonicity for this mode, quite comparable with that of ZnH^+. The ν_1 values of $H^{64}ZnF$ and $H^{64}Zn^{35}Cl$ only differ by 40 cm^{-1}, emphasizing the little dependence on the halogen atom in the ZnH stretching mode as also confirmed by the data in Table 5.

The bending and the ZnF stretching modes of HZnF are also almost harmonic with $\nu_2 = 474.5$ cm^{-1}, $2\nu_2{}^0$ ($|K| = 2$) = 938.6 cm^{-1}, $\nu_3 = 684.8$ cm^{-1}, and $2\nu_3 = 1360.8$ cm^{-1}. The rotational constant $B_{000} = 0.3540$ cm^{-1}, from variational calculations, is coherent with $B_e = 0.3561$ cm^{-1} from the calculated equilibrium geometry. These values are twice larger than $B_{000} = 0.162\,031\,25$ and $0.163\,397\,060$ cm^{-1} for $H^{64}Zn^{35}Cl$ measured by Yu et al.[12] and Pulliam et al.,[13] respectively.

6. Conclusions

The electronic structure and spectroscopic properties of the ground state of HZnF have been revealed for the first time in this study, based on its potential energy surface obtained at the MRCI+Q and CCSD(T) levels. Our results have been compared with those of the close system HZnCl, which were reported in recent works.[12−14] Even though we focus on the $X^1\Sigma^+$ electronic ground state, many excited states should be included in the MCSCF calculations. For this ionic molecule, it is essential to take into account the interactions between the close lying states for an accurate description, indeed, this process has required many computational efforts. We have also determined the rovibrational energy levels of the $X^1\Sigma^+$ state. From the study of the potential curves and of some spectroscopic properties of the electronic ground states of ZnH and ZnH^+, we could deduce that the H−Zn bond in HZnF is found to be quite similar to those in HZnCl and in the ZnH^+ cation. According to the rotational constant and to the different harmonic frequencies of ω_2 and ω_3, the vibration−rotation spectrum of the ground state of HZnF is expected to be different from the one of HZnCl.

The experimental difficulties in the spectroscopy of HZnCl due to the presence of ZnCl in the mixture and to the existence of many Zn isotopologues are similarly expected for HZnF. However, using the present results, HZnF would be a likely target for pure vibrational as well as rovibrational experimental studies. Note that the PES data are available upon request.

References and Notes

(1) Li, Y.; Xi, G. *J. Hazard. Mat.* **2005**, *B127*, 244.
(2) Liao, G.; Chen, Q.; Xing, J.; Gebavi, H.; Milanese, D.; Fokine, M.; Ferraris, M. *J. Non-Cryst. Solids* **2009**, *355*, 447.
(3) Greenwood, N. N.; Earnshaw, A. *Chemistry of the Elements*, 2nd ed.; Butterworth: Heinemann, Linacre House, Jordan Hill, Oxford, 1997.
(4) Davies, M. A.; Lindsay, D. M. *Surf. Sci.* **1985**, *156*, 335.
(5) Lindsay, D. M.; Symons, M. C. R.; Herschbach, D. R.; Kwiram, A. L. *J. Phys. Chem.* **1982**, *86*, 3789.
(6) Kasai, P. H. *J. Phys. Chem. A* **2000**, *104*, 4514.
(7) Parker, S. F.; Peden, C. H. F.; Barrett, P. H.; Pearson, R. G. *J. Am. Chem. Soc.* **1984**, *106*, 1304.
(8) Legay-Sommaire, N.; Legay, F. *Chem. Phys. Lett.* **1999**, *314*, 40.
(9) Legay-Sommaire, N.; Legay, F. *J. Phys. Chem.* **1995**, *99*, 16945.
(10) Köppe, R.; Kasai, P. H. *J. Am. Chem. Soc.* **1996**, *118*, 135.
(11) Macrae, V. A.; Green, J. C.; Greene, T. M.; Downs, A. J. *J. Phys. Chem. A* **2004**, *108*, 9500.
(12) Yu, S.; Shayesteh, A.; Fu, D.; Bernath, P. F. *J. Phys. Chem. A* **2005**, *109*, 4092.
(13) Pulliam, R. L.; Sun, M.; Flory, M. A.; Ziurys, L. M. *J. Mol. Spectrosc.* **2009**, *257*, 128.
(14) Kerkines, I. S. K.; Mavridis, A.; Karipidis, P. A. *J. Phys. Chem. A* **2006**, *110*, 10899.
(15) Emsley, J. *The Elements*, Second ed.; Oxford University Press, 1989.
(16) Huber, K. P.; Herzberg, G. *Molecular Spectra and Molecular Structure, Vol. IV, Constants of Diatomic Molecules*; Van Norstrand Reinhold: New York, 1979.
(17) Stenvinkel, G. Earlier work reviewed in ref 16, 1936.
(18) Hayashi, S.; Léonard, C.; Chambaud, G. *J. Chem. Phys.* **2008**, *129*, 044313.
(19) Moore, Ch. E. *Atomic Energy Levels, Vol. I-II*; Circular of the National Bureau of Standards 467; U.S. Government Printing Office: Washington, DC, 1949.
(20) Bengtsson, E.; Grundström, B. *Z. Phys.* **1929**, *57*, 1.
(21) Moravec, V. D.; Klopcic, S. A.; Chatterjee, B.; Jarrold, C. C. *Chem. Phys. Lett.* **2001**, *341*, 313.
(22) Figgen, D.; Rauhut, G.; Dolg, M.; Stoll, H. *Chem. Phys.* **2005**, *311*, 227.
(23) Peterson, K. A.; Puzzarini, C. *Theor. Chem. Acc.* **2005**, *114*, 283.
(24) Bergner, A.; Dolg, M.; Kuchle, W.; Stoll, H.; Preuss, H. *Mol. Phys.* **1993**, *80*, 1431.
(25) Dunning, T. H., Jr. *J. Chem. Phys.* **1989**, *90*, 1007.
(26) Kendall, R. A.; Dunning, T. H., Jr.; Harrison, R. J. *J. Chem. Phys.* **1992**, *96*, 6769.
(27) Werner, H.-J.; Knowles, P. J. *J. Chem. Phys.* **1985**, *82*, 5053.
(28) Knowles, P. J.; Werner, H.-J. *Chem. Phys. Lett.* **1985**, *115*, 259.
(29) Werner, H.-J.; Knowles, P. J. *J. Chem. Phys.* **1988**, *89*, 5853.
(30) Knowles, P. J.; Werner, H.-J. *Chem. Phys. Lett.* **1988**, *145*, 514.
(31) Langhoff, S. R.; Davidson, E. R. *Int. J. Quantum Chem.* **1974**, *8*, 61.
(32) Blomberg, M. R. A.; Siegbahn, P. E. M. *J. Chem. Phys.* **1983**, *78*, 5682.
(33) *MOLPRO, a Package of Ab Initio Programs*, version 2006 Werner, H.-J.; Knowles, P. J.; Lindh, R.; Manby, F. R.; Schütz, M. and others, see http://www.molpro.net.
(34) Berning, A.; Schweizer, M.; Werner, H.-J.; Knowles, P. J.; Palmieri, P. *Mol. Phys.* **2000**, *98*, 1823.
(35) Hampel, C.; Peterson, K.; Werner, H.-J. *Chem. Phys. Lett.* **1992**, *190*, 1.
(36) Deegan, M. J. O.; Knowles, P. J. *Chem. Phys. Lett.* **1994**, *227*, 321.
(37) Lee, T. J.; Taylor, P. R. *Int. J. Quantum Chem. Symp.* **1989**, *23*, 199.
(38) Senekowitsch, J., et al. SURFIT; Ph. D. Thesis, Johan Wolfgang Goethe Universität; Frankfurt-am-Main, Germany, 1988.
(39) Carter, S.; Handy, N. C.; Puzzarini, C.; Tarroni, R.; Palmieri, P. *Mol. Phys.* **2000**, *98*, 1697.
(40) Jamorski, Ch.; Dargelos, A.; Teichteil, Ch.; Daudey, J. P. *J. Chem. Phys.* **1994**, *100*, 917.
(41) Chong, D. P.; Langhoff, S. R. *J. Chem. Phys.* **1986**, *84*, 5606.
(42) Chong, D. P.; Langhoff, S. R.; Bauschlicher, Ch. W., Jr.; Walch, S. P.; Partridge, H. *J. Chem. Phys.* **1986**, *85*, 2850.
(43) Shayesteh, A.; Le Roy, R. J.; Varberg, T. D.; Bernath, P. F. *J. Mol. Spectrosc.* **2006**, *237*, 87.
(44) Urban, R.-D.; Magg, U.; Brik, H.; Jones, H. *J. Chem. Phys.* **1990**, *92*, 14.
(45) Khan, M. S. *Proc. Phys. Soc.* **1962**, *80*, 599.
(46) Schilling, J. B.; Goddar III, W. A.; Beauchamp, J. L. *J. Am. Chem. Soc.* **1986**, *108*, 582.
(47) Greene, T. M.; Brown, W.; Andrews, L.; Downs, A. J.; Chertihin, G. V.; Runeberg, N.; Pyykkö, P. *J. Phys. Chem.* **1995**, *99*, 7925.
(48) Senekowitsch, J. *NUMEROV Algorithm Code*; Johan Wolfgang Goethe Universität: Frankfurt-am-Main, Germany, 1989.
(49) Flory, M. A.; McLamarrah, S. K.; Ziurys, L. M. *J. Chem. Phys.* **2006**, *125*, 194304.
(50) Tenenbaum, E. D.; Flory, M. A.; Pulliam, R. L.; Ziurys, L. M. *J. Mol. Spectrosc.* **2007**, *244*, 153.

JP9043607